

# Sensors & Diagnostics

Volume 3  
Number 11  
November 2024  
Pages 1761–1878

rsc.li/sensors



ISSN 2635-0998



**PAPER**

Shalini Prasad *et al.*

Development of a portable electrochemical sensing platform for impedance spectroscopy-based biosensing using an ARM-based microcontroller


Cite this: *Sens. Diagn.*, 2024, **3**, 1835

## Development of a portable electrochemical sensing platform for impedance spectroscopy-based biosensing using an ARM-based microcontroller†

Joseph Charles Khavul Spiro,<sup>‡a</sup> Kundan Kumar Mishra,<sup>‡a</sup>  
Vikram Narayanan Dhamu,<sup>b</sup> Avi Bhatia,<sup>a</sup>  
Sriram Muthukumar <sup>b</sup> and Shalini Prasad <sup>\*ab</sup>

Detecting pesticides like atrazine is a significant global health challenge due to their association with numerous foodborne illnesses. Traditional detection methods often lack sensitivity and time efficiency, highlighting the urgent need for improved early detection techniques to mitigate pesticide contamination and outbreaks. This study introduces a novel portable electrochemical prototype that integrates an ARM-based microcontroller with an impedance spectroscopy (EIS)-based biosensing system. The data processed through the algorithm generates easily interpretable impedance values. The platform demonstrates a broad detection range for atrazine (1 fg mL<sup>-1</sup> to 10 ng mL<sup>-1</sup>) with a limit of detection (LoD) of 1 fg mL<sup>-1</sup> and an assay processing time of approximately 5 minutes, showcasing its remarkable efficiency. The sensor consistently maintains cross-reactivity variation below 20%, ensuring reliable performance. This research aims to offer a low-cost, replicable mobile platform for biosensing applications, thereby enhancing access for individuals with limited lab-based research experience and broadening the scope of proactive pesticide monitoring.

Received 2nd July 2024,  
Accepted 19th August 2024

DOI: 10.1039/d4sd00234b

rsc.li/sensors

## 1. Introduction

Pesticides are necessary for modern agriculture, which guards plants against damage by insects or animals thereby maintaining food security. But their extensive application results into pollution of air, water, soil and foodstuffs thus creating serious environmental problems as well as human health risks due to the presence of persistent residues of these chemicals.<sup>1</sup> Atrazine (2-chloro-4-(ethylamino)-6-(isopropylamino)-s-triazine) is among the most used herbicides because it has high effectiveness against weeds coupled with low cost; however, this pesticide is worrisome on account of its long half-life combined with high potential contamination of groundwaters.<sup>2</sup> The compound may persist in soils due to strong adsorption onto clay particles or organic matter surfaces but also move downward through leaching depending on rainfall intensity and soil type. Atrazine's

high soil mobility and moderate water solubility, combined with its lengthy half-life of 57 weeks, increase the risk of groundwater contamination.<sup>3,4</sup> Exposure to atrazine has been linked with various reproductive abnormalities, developmental problems and endocrine disrupting diseases while some studies have indicated that it may also have carcinogenic effects.<sup>5,6</sup> The maximum contaminant level (MCL) set by the US Environmental Protection Agency (EPA) for drinking water is 3.0 ng mL<sup>-1</sup> showing the importance of precise low level detection method development. Conventional methods, such as high performance liquid chromatography with UV-visible detection (HPLC-UV), gas chromatography mass spectrometry (GC MS), enzyme linked immunosorbent assay (ELISA), *etc.*, are available but they are expensive, laborious and require extensive sample clean up making them unsuitable for on-site real time remote monitoring systems without logistical support like inter laboratory transport logistics involving field work across different isolated research facilities worldwide endowed with refrigerated storages for preservation of stability pending analysis.

To develop biosensors for atrazine, the limitations of traditional methods have been recognized. These biosensors should produce results quickly, should be easy to use, highly sensitive and selective with respect to atrazine only, and also cost-effective so that many can be located on site for real time

<sup>a</sup> Department of Bioengineering, University of Texas at Dallas, Richardson, TX 75080, USA. E-mail: shalini.prasad@utdallas.edu

<sup>b</sup> EnLiSense LLC, 1813 Audubon Pondway, Allen, TX 75013, USA

† Electronic supplementary information (ESI) available. See DOI: <https://doi.org/10.1039/d4sd00234b>

‡ Equal contribution.



monitoring where only limited volumes of waste would be generated.<sup>7–19</sup> To date, there is no solution found despite checking several systems such as BIAcore<sup>7</sup> or integrated optical grating coupler sensor BIOS – 1 made by ASI company.<sup>8</sup> Others have employed laboratory models which achieved the desired low detection limits using impedimetric devices<sup>14,16–18</sup> among other examples like waveguide based SPRs<sup>13</sup> but this was only for testing with standard solutions. The development of immunosensors also needs stable and reproducible immobilization of many antibodies on their transducer surfaces while retaining biological activities which are essential for commercial biosensor development.<sup>20,21</sup> Many such devices utilize conductive platforms coated with electrogenerated polymeric films where electro-polymerization gives rise to defect free water/organic solvent stable homogeneous films thus providing molecular level homogeneous biomolecule attachment sites.<sup>22,23</sup> Table S1† offers a comparative examination of different immunosensors, indicating that label-free versions lack the necessary sensitivity for directly detecting atrazine.

Our platform integrates portable electrochemical sensors designed for efficient field deployment. Utilizing the STMicroelectronics 32-bit microcontroller (STM32) Nucleo – F303RE Advanced RISC (reduced instruction set computing) Machine (ARM) microcontroller with a 12-bit digital-to-analog converter (DAC) and analog-to-digital converter (ADC), and AD8605 amplifiers, it ensures accurate signal processing. Electrochemical impedance spectroscopy (EIS) measurements are facilitated using a Gamry Randles cell, converting antigen-antibody interactions specific to atrazine into measurable non-faradaic signals. Impedance calculations follow  $Z = V/I$ , where raw ADC values are converted into voltage ( $V$ ) and current ( $I$ ). Specifically, Voltage = (max/resolution of ADC)  $\times$  3.3 V and

Current = ((max1/resolution of ADC)  $\times$  3.3 V)/24 000 (sense resistor). Moreover, our matrix laboratory (MATLAB) script facilitates phase and impedance calculations, incorporating a sophisticated noise rejection algorithm to enhance signal clarity. This streamlined approach not only ensures timely and sensitive detection but also eliminates the need for extensive preprocessing or specialized laboratory infrastructure, thereby making our platform ideal for real-world applications. Fig. 1 depicts the schematic of our modified sensor platform for electrochemical detection of atrazine, highlighting its robust integration of hardware and software components.

## 2. Materials and methods

### 2.1 Materials and reagents

The polyclonal atrazine antibodies were obtained from Invitrogen (USA), while heat-killed atrazine cells were sourced from Cedarlane as the native antigen. Phosphate buffered saline (PBS) with a pH of 7.4 and 3,3'-dithiobis(sulfosuccinimidyl propionate) were purchased from Thermo Fisher Scientific Inc. These reagents were aliquoted and stored at  $-20\text{ }^{\circ}\text{C}$  until required for experimentation. Before use, the small samples were thawed to room temperature and then centrifuged to ensure uniformity. Throughout this study, high-purity chemicals were employed, which obviated the need for any additional purification steps prior to their application.

### 2.2 System architecture/hardware setup

The experimental setup employed an ARM microcontroller, specifically the STM32 Nucleo – F303RE, chosen for its high clock speed and extensive peripheral capabilities. This board features a 12-bit DAC for precise digital-to-analog signal

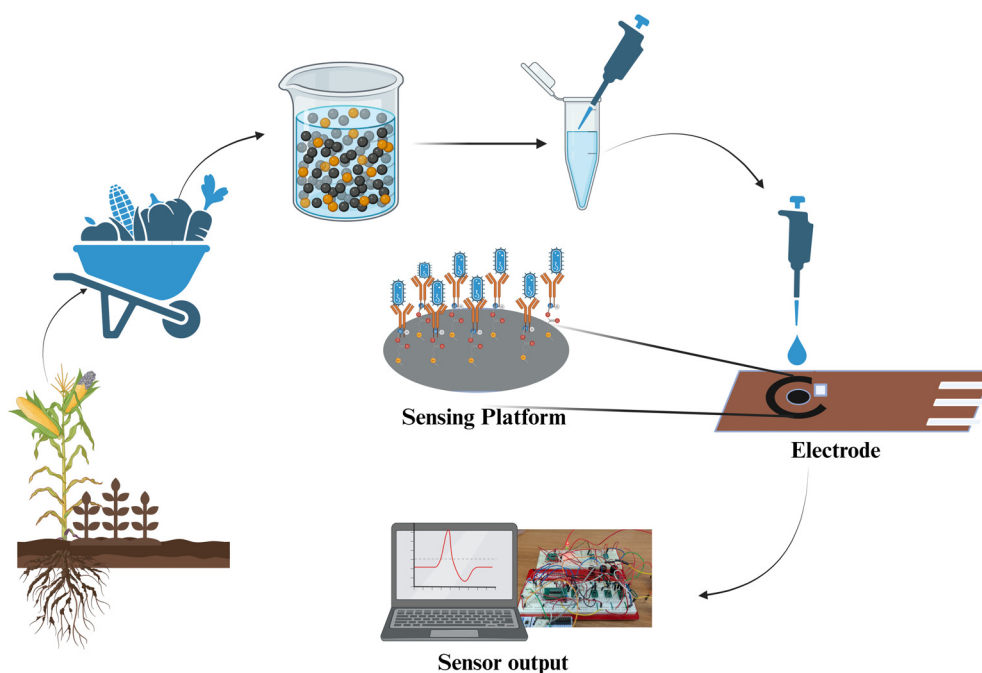


Fig. 1 Schematic of the electrochemical detection of atrazine on the modified sensor platform.





conversion and an ADC for accurate analog-to-digital data collection. Additionally, multiple AD8605 amplifiers were utilized along with a Gamry universal dummy cell 4 (Randles cell) as a standardized load for electrochemical impedance spectroscopy (EIS) evaluation. EIS involved injecting a sinusoidal signal of fixed frequency and amplitude into the load, followed by collection of the resultant current output to calculate impedance. The onboard DAC generated a 0–3.3 volt signal, attenuated to a 100 mV amplitude, which was then captured by the first ADC with an offset for signal conditioning before being fed into the sensing circuit and Randles cell using the reference electrode. A current sensing shunt resistor, crucial for sensing resolution, was employed, and a second ADC captured the voltage after the shunt (high-side sensing), adjusted to a positive regime. Fig. 2 illustrates the hardware configuration of the ARM microcontroller-based platform. The system utilized a feedback loop in the sensing circuit to achieve a steady state and conducted subtraction operations to maintain output stability at the working electrode potential, ensuring consistent impedance measurements and graph generation.

### 2.3 Software

The MATLAB script developed for this sensor system performs phase and impedance calculations to generate graphs from input and output data. The script processes sinusoidal input and output waveforms by identifying their maximum data points and calculating phase differences. Specifically, a loop iterates through the data to determine these points, computes the phase shift using their indices and waveform periods, and converts it into degrees ( $360^\circ \times (\text{maxindex1} - \text{maxindex2})/(\text{period})$ ). Additionally, the script integrates a noise rejection algorithm based on a moving average equation, which enhances data clarity by averaging every ten data points and smoothing the resulting curves.

Data alignment is crucial for accurate geometric phase and magnitude calculations. Our approach involves centering both input and output waveforms around zero using MATLAB functions, achieved by adjusting each data point relative to the midpoint between the minimum and maximum values. Phase calculations are refined by pinpointing the first local maxima of each waveform and computing their index difference over the waveform period, converted into degrees. The MATLAB script utilized a moving average noise rejection formula that smoothens a signal and reduces noise by comparing values within a sliding window. This window, normally three to five data points, took the average of the data points within the window, allowing for the rejection of extreme points and noise, while maintaining the signal. This can be compared to circuit-based elements, like attenuators and a high-bandpass, which were used before and after the onboard ADC and DACs.

Impedance calculations commence with converting raw ADC values to input voltage ( $V$ ) and output current ( $I$ ) in a 3.3-volt system. The input voltage equation is calculated as  $\text{Voltage} = (\text{max}/\text{resolution of ADC}) \times 3.3 \text{ V}$ , where 'max' denotes the peak index of the input waveform. The current output is calculated as  $\text{Current} = ((\text{max1}/\text{resolution of ADC}) \times 3.3 \text{ V})/24\,000$  (sense resistor), using 'max1' for the output waveform peak index and a sense resistor value of 24 000 ohms. Impedance magnitude is derived from  $Z = \sqrt{(\tan(\text{phase})^2) + (V/I)^2}$ , integrating phase and voltage-current ratio calculations. Fig. 3 illustrates the comprehensive circuit diagram, detailing interactions between the STM32 microcontroller and the Randles cell, central to our experimental setup.

### 2.4 Modification of the sensing platform and electrochemical studies

The sensor is built on a small printed circuit board (PCB) using a two-electrode system, with a gold working electrode enhanced by a zinc oxide (ZnO) coating applied through electron vapor deposition.<sup>24</sup> The inclusion of ZnO is crucial as it increases the surface area and provides a biocompatible interface for the

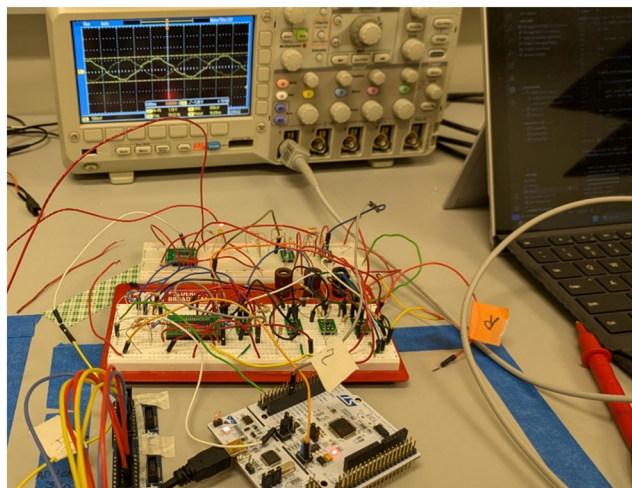


Fig. 2 Image showing a wide view of the constructed board, power supply, and environment-controlled housing for sensors.

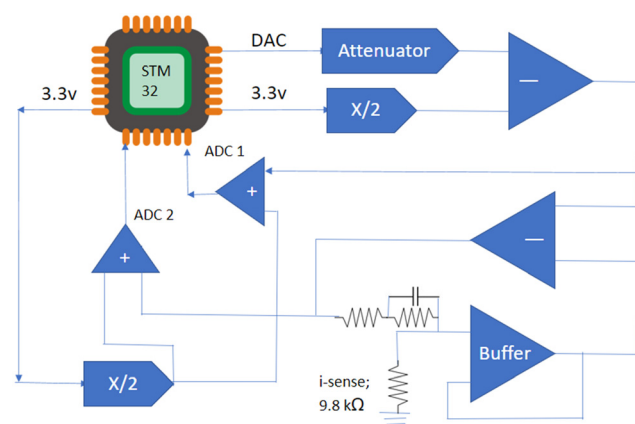


Fig. 3 Block diagram of the circuit in relation to STM32 and the Randles cell.



immobilization of antibodies, thereby enhancing the sensor's sensitivity and specificity for atrazine detection. To modify the sensor for atrazine detection, we initially cleansed the sensor surface using phosphate-buffered saline (PBS) to ensure it was free from contaminants. Following this, we prepared a solution containing 10 mM dithiobis(sulfosuccinimidyl propionate) (DTSSP) and  $10\ \mu\text{g mL}^{-1}$  antibodies. This solution was meticulously applied to the sensor surface, ensuring an even coating. The sensor was then incubated at  $4\ ^\circ\text{C}$  for 30 minutes to facilitate the binding of the antibodies to the crosslinker on the sensor surface. After the incubation period, the sensor was thoroughly rinsed with PBS to remove any unbound reagents, ensuring that only the antibodies firmly attached to the sensor surface remained. Subsequently,  $20\ \mu\text{L}$  of the sample was applied to the modified sensor surface. This sample was incubated for an additional 5 minutes to allow sufficient interaction between the sample components and the modified sensor surface. Electrochemical impedance spectroscopy (EIS) was employed to assess the interactions on the sensor surface. The impedance response was recorded using a  $10\ \text{mV}$  AC bias across a frequency range of  $1000\ \text{Hz}$  to  $80\ \text{Hz}$ . Before conducting these measurements, calibration was performed using the Gamry dummy cell. This step involved using standard solutions of known atrazine concentrations to validate the sensor's performance, ensuring high accuracy and reliability in the data obtained. This calibration procedure enabled the successful

functionalization of the sensor platform and provided detailed information about its electrochemical properties.

### 3. Results and discussion

#### 3.1 Sensor characterization

In our study, we investigated atrazine detection through affinity-based functionalization. Initially, a thiol-based crosslinker, DTSSP, was chemically attached to the electrode surface, followed by the immobilization of atrazine antibodies onto the DTSSP-modified surface. Fig. 4A provides a simplified illustration of the potential distribution within the electric double layer (EDL), which comprises the stern layer, where ions and molecules strongly adhere to the electrode surface, and the diffuse layer, where ions are more loosely bound beyond the stern layer.<sup>25</sup> The interactions between atrazine antibodies and antigens on the electrode surface result in alterations in the EDL, as depicted in Fig. 4B, which shows schematic images of our sensor platform. To validate our functionalization process, atomic force microscopy (AFM) was employed. The AFM topographic images in Fig. 4C and D reveal the sensor surface before and after modification, showing the presence of antibodies measuring approximately  $300\text{--}450\ \text{nm}$  adhering to the crosslinker on the sensor platform.<sup>26</sup> These observations confirm that our sensor is functional and efficient in detecting

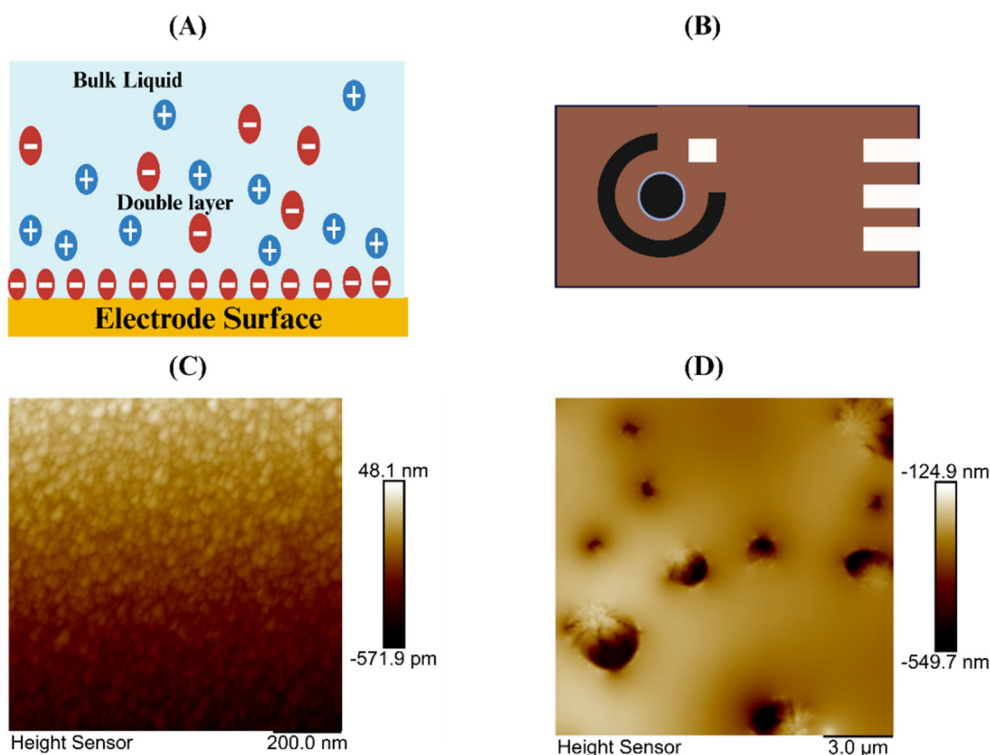


**Fig. 4** Various aspects of the sensor platform. Panel (A) illustrates a schematic representation depicting how the interaction between the antigen and the antibody-modified platform induces alterations in the double layer at the electrode–electrolyte interface. Panel (B) shows a schematic image of the sensor platform itself. Panel (C) provides an atomic force microscopy (AFM) image, revealing the surface characteristics of the sensor platform. Finally, panel (D) displays the sensor surface after it has been modified with the antibody and crosslinker, thereby confirming the presence of these components on the sensor surface.



atrazine pesticide with high accuracy and sensitivity, indicating its significant potential for practical applications.

### 3.2 Electrochemical impedance spectroscopy (EIS) for atrazine detection

Electrochemical impedance spectroscopy (EIS) was utilized to assess the electrochemical performance of a custom sensor specifically designed for the detection of atrazine pesticide. This advanced methodology involved conducting electrochemical measurements with EIS, applying a 10 mV AC bias.<sup>24,27,28</sup> The observed signal variations resulted from shifts in the electrical charge on the sensor surface,<sup>29</sup> which occurred when the target antigen attached to the immobilized antibodies, as illustrated in Fig. 5A. This process facilitated highly accurate and sensitive detection of atrazine pesticide, thereby enhancing the sensor's utility for applications in medical diagnostics and environmental monitoring. To create calibrated dose response

(CDR) plots for varying antigen concentrations, impedance changes were meticulously tracked and atrazine antigen doses were generated by serial dilution, starting at zero (control matrix) and going up to quantities of 1 fg mL<sup>-1</sup>, 10 fg mL<sup>-1</sup>, 100 fg mL<sup>-1</sup>, and 10 ng mL<sup>-1</sup>. Phosphate-buffered saline (PBS) matrices were used for these studies in order to fully assess the sensor's response over a wide concentration range.

The EIS measurement results yielded a dose-dependent plot illustrating how impedance ( $Z_{mod}$ ) varied with different amounts of atrazine antigen. Impedance values increase as the concentration of atrazine increases, as depicted in Fig. 5B. Stronger antigen binding was indicated by a linear association between antigen concentrations and impedance, which changed the double-layer charge and resulted in signal variations across a broad frequency range. The peak signal-to-noise ratio was perfect for producing and assessing the calibrated dose-response plot because it was detected at a lower frequency.<sup>30,31</sup> This investigation provided valuable insights into the sensor's

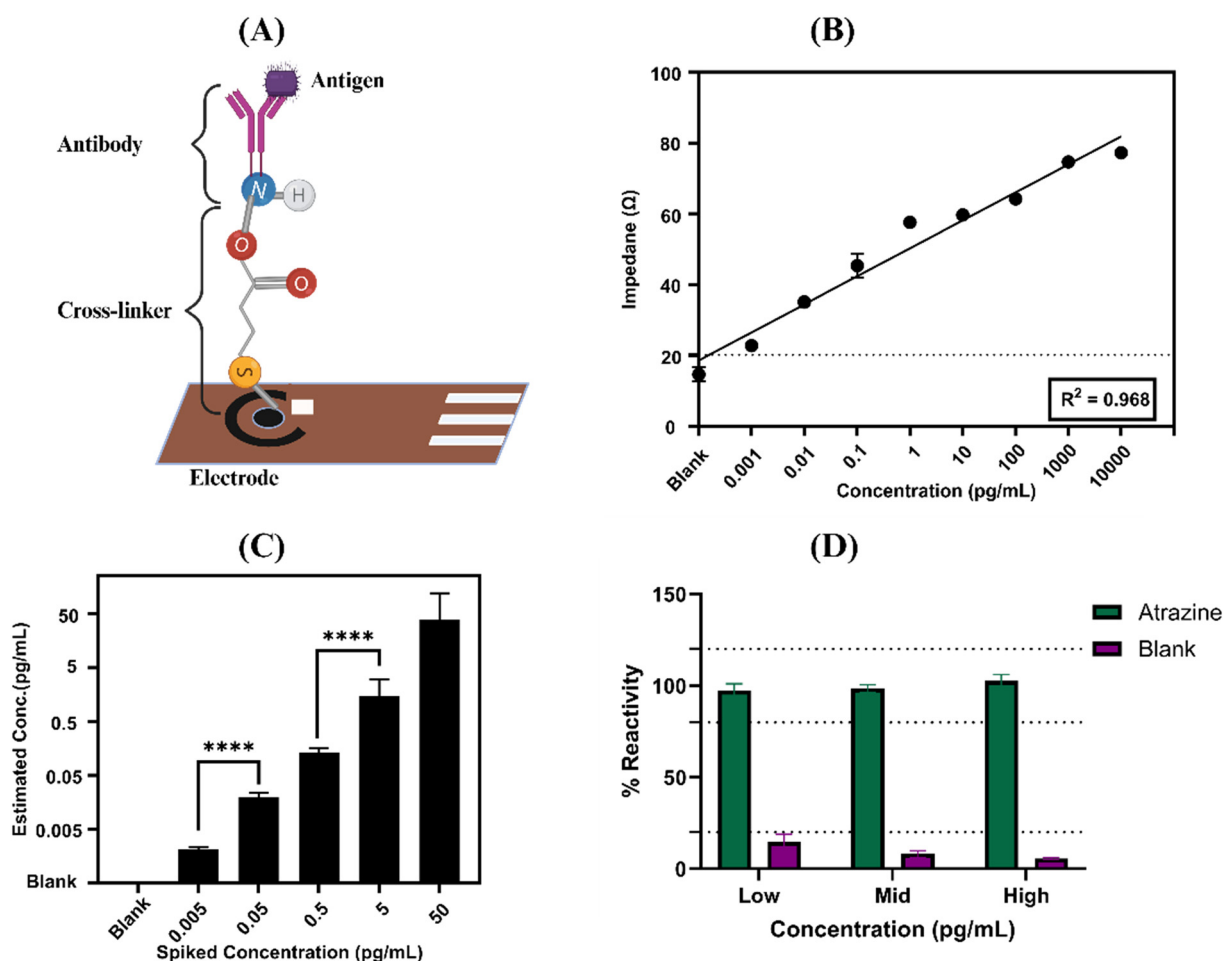


Fig. 5 Detailed depiction of the sensor platform's functionality and performance. Panel (A) illustrates a schematic representation of the immobilization process, where linker molecules are attached to the sensor substrate and antibodies are covalently conjugated to these linkers. Panel (B) displays a calibration dose response (CDR) for atrazine, showing sensor responses across various concentrations: 1 fg mL<sup>-1</sup>, 10 fg mL<sup>-1</sup>, 100 fg mL<sup>-1</sup>, 1 pg mL<sup>-1</sup>, 10 pg mL<sup>-1</sup>, 100 pg mL<sup>-1</sup>, 1 ng mL<sup>-1</sup>, and 10 ng mL<sup>-1</sup>. Panel (C) illustrates the signal response of the sensor platform to spiked dose concentrations ranging from 5 fg mL<sup>-1</sup> to 50 pg mL<sup>-1</sup> in PBS and paired *t*-test results (\*\*\*\* represents the significant difference between the low to mid concentration and mid to high concentration readings). Lastly, panel (D) presents the results of the specificity study, highlighting the sensor's response to increasing concentrations of atrazine compared to a blank control.



sensitivity and dynamic range. In Fig. 5B, a representative CDR plot is presented, featuring a specific signal threshold (SST) used to distinguish signal from noise.<sup>32</sup> This cutoff was determined by multiplying the blank's standard deviation (SD) by three and adding it to the blank concentration's mean (ZD). Significant variations in the electrical double layer (EDL) were seen when more antigen was added, suggesting that the electrical characteristics at the interface level had changed. These changes, which represented interactions between antigens and antibodies, were directly linked to bonding activities between biomolecules.

Our thorough investigation confirmed that our immunoassay was successful in identifying antigens and offered important new information about the electrochemical mechanisms underlying these interactions. This validation highlights the sensor's potential for practical applications in various fields, reinforcing its reliability and efficiency in detecting atrazine pesticide.

### 3.3 Spike and recovery study

An established analytical approach used to assess the precision and dependability of measuring methods is the spike and recovery methodology. In this study, we utilized this technique by adding known concentrations of atrazine to samples and calculating the percentage recovery using the calibrated dose response (CDR), as illustrated in Fig. 5B. This method is crucial for assessing the precision and bias of our analytical procedure by comparing the expected concentration (the spike) with the measured concentration. Atrazine was introduced into the samples at various concentrations, ranging from the control (zero concentration) to 5 fg mL<sup>-1</sup>, 50 fg mL<sup>-1</sup>, 500 fg mL<sup>-1</sup>, 5 pg mL<sup>-1</sup>, and 50 pg mL<sup>-1</sup>. By utilizing the CDR, we were able to determine the recovery rates for these concentrations. The experiments included four replicates ( $N = 4$ ), ensuring robustness and reliability of the data. The percentage recovery plot in phosphate-buffered saline (PBS) is depicted in Fig. 5C. Across these different concentrations, the percentage error consistently remained below 20%, indicating a strong correlation between the sensor's readings and the actual atrazine concentrations in PBS.<sup>33</sup> Furthermore, the sensor's limit of detection (LoD) was determined to be an impressively low 1 fg mL<sup>-1</sup>, achieved using the signal-to-noise (S/N) threshold method. This result underscores the sensor's capability to detect very low levels of atrazine contamination. The ability to maintain high accuracy and reliability in measuring atrazine concentrations, even at such minute levels, highlights the sensor's exceptional performance and suitability for sensitive analytical applications. Furthermore, the paired *t*-test was conducted on the data to analyze significant differences between the doses, as illustrated in Fig. 5C. The results of the paired *t*-test revealed a significant difference between the readings of low to mid concentration and mid to high concentration for the portable device ( $p$ -value = 0.0001). This consistency underscores the reliability

of both instruments for accurate assessments across various applications, ensuring confidence in their usage.

### 3.4 Cross reactivity

For a sensor platform to function well and be dependable, it must be effective, particularly in real-time applications. The sensor matrix and electrode are exposed to a wide range of nutrients in real-world situations, which may have an impact on the binding of minerals and nutrients. Additionally, the presence of structurally similar pesticides at higher concentrations can further complicate data interpretation. To address these challenges, we conducted a comprehensive cross-reactivity test to evaluate the modified sensor platform's response to various concentrations of cross-reactive antigens alongside the primary analytes in phosphate-buffered saline (PBS). The details of this test are illustrated in Fig. 5D. The response plot, which focuses on detecting atrazine in PBS, demonstrates that there is less than 20% change in total impedance after the exposure of blanks on the atrazine-antibody sensor platform.<sup>34</sup> These findings underscore the high specificity of our sensor platform, indicating minimal cross-reactivity even at varying concentrations of structurally similar compounds. To evaluate how the sensor platform interacts with other pesticides, we tested both atrazine and glyphosate at the same concentrations on the sensor. Our thorough analysis revealed that glyphosate exhibits minimal cross-reactivity with the atrazine sensor platform, showing a response of less than 20%. This finding indicates that glyphosate has a negligible effect on the sensor's accuracy in detecting atrazine, confirming that the sensor maintains a high level of specificity even when other substances are present. Details of this cross-reactivity study are illustrated in ESI† Fig. S1. For accurate pesticide identification in real-world water samples, where the presence of many chemicals and other pollutants might confound the study, this degree of selectivity is crucial. The usability and reliability of the sensor platform in real-world applications are greatly increased by its capacity to discriminate between target analytes and cross-reactive antigens. As a result, the sensor is extremely well-suited for field deployment in a variety of climatic circumstances, guaranteeing precise and trustworthy data in a wide range of real-world situations.

## 4. Conclusion

This study demonstrates the efficacy of a novel electrochemical impedance spectroscopy (EIS) platform for the swift and reliable detection of atrazine in PBS. By integrating an ARM-based microcontroller and a simple sensing circuit, the sensor's selectivity is significantly enhanced, enabling precise identification of target antigens. Our system facilitates rapid detection, delivering results in less than 5 minutes with a minimal sample volume of just 20 µL. The sensor achieves an impressive limit of detection (LoD) of 1 fg mL<sup>-1</sup> for atrazine and consistently performs across both laboratory settings and portable device applications, covering a wide concentration range from 1 fg mL<sup>-1</sup> to 10 ng mL<sup>-1</sup>. Extensive cross-reactivity





testing has confirmed the sensor platform's specificity. Notably, this platform utilizes non-faradaic EIS, eliminating the need for a redox tag and sample pre-preparation, thereby simplifying the detection process. This electrochemical-based sensing platform offers a promising approach for pesticide detection in PBS samples. Its portable and user-friendly design makes it well-suited for field-deployable monitoring, enabling prompt identification of pesticide contamination in PBS water. The research outcomes are crucial for advancing electrochemical sensing platforms, contributing significantly to the mitigation of contamination and maintaining PBS sanitation standards. By addressing key challenges in atrazine detection, these findings play a vital role in ensuring public health and hygiene. Moreover, this work stands out by combining the simplicity and portability of the sensor with high sensitivity and rapid detection capabilities, making it a competitive and practical solution compared to other recently reported methods and strategies for developing portable immunosensors.

## Data availability

Data supporting the reported results are contained within the article. No new data were created beyond those presented in the study.

## Conflicts of interest

The authors declare the following financial interests/personal relationships which may be considered as potential competing interests: Drs. Shalini Prasad and Sriram Muthukumar have a significant interest in Enlisen LLC, a company that may have a commercial interest in the results of this research and technology. The potential individual conflict of interest has been reviewed and managed by The University of Texas at Dallas, and played no role in the study design; in the collection, analysis, and interpretation of data; in the writing of the report, or in the decision to submit the report for publication. Portable device and technology platform is a proprietary of EnLiSense LLC.

## References

- 1 P. Pichetsurnthorn, K. Vattipalli and S. Prasad, Nanoporous impedimetric biosensor for detection of trace atrazine from water samples, *Biosens. Bioelectron.*, 2012, **32**, 155–162.
- 2 V. N. Dhamu, D. C. Poudyal, C. M. Telang, A. Paul, S. Muthukumar and S. Prasad, Electrochemically mediated multi-modal detection strategy-driven sensor platform to detect and quantify pesticides, *Electrochem. Sci. Adv.*, 2022, **2**(6), e2100128.
- 3 J. Chang, W. Fang, L. Chen, P. Zhang, G. Zhang, H. Zhang, J. Liang, Q. Wang and W. Ma, Toxicological effects, environmental behaviors and remediation technologies of herbicide atrazine in soil and sediment: A comprehensive review, *Chemosphere*, 2022, **307**, 136006.
- 4 J. L. Rinsky, C. Hopenhayn, V. Golla, S. Browning and H. M. Bush, Atrazine exposure in public drinking water and preterm birth, *Public Health Rep.*, 2012, **127**, 72–80.
- 5 E. Pérez-Carrera, V. M. L. León, A. G. Parra and E. González-Mazo, Simultaneous determination of pesticides, polycyclic aromatic hydrocarbons and polychlorinated biphenyls in seawater and interstitial marine water samples, using stir bar sorptive extraction-thermal desorption-gas chromatography-mass spectrometry, *J. Chromatogr. A*, 2007, **1170**, 82–90.
- 6 K. E. Hyer, G. M. Hornberger and J. S. Herman, Processes controlling the episodic streamwater transport of atrazine and other agrichemicals in an agricultural watershed, *J. Hydrol.*, 2001, **254**, 47–66.
- 7 M. Minunni and M. Mascini, Detection of Pesticide in Drinking Water Using Real-Time Biospecific Interaction Analysis (BIA), *Anal. Lett.*, 1993, **26**, 1441–1460.
- 8 F. F. Bier and R. D. Schmid, Real time analysis of competitive binding using grating coupler immunosensors for pesticide detection, *Biosens. Bioelectron.*, 1994, **9**, 125–130.
- 9 R. G. Heideman, R. P. H. Kooyman and J. Greve, Performance of a highly sensitive optical waveguide Mach-Zehnder interferometer immunosensor, *Sens. Actuators, B*, 1993, **10**, 209–217.
- 10 C. Mouvet, R. D. Harris, C. Maciag, B. J. Luff, J. S. Wilkinson, J. Piehler, A. Brecht, G. Gauglitz, R. Abuknesha and G. Ismail, Determination of simazine in water samples by waveguide surface plasmon resonance, *Anal. Chim. Acta*, 1997, **338**, 109–117.
- 11 G. G. Guibault, B. Hock and R. Schmid, A piezoelectric immunobiosensor for atrazine in drinking water, *Biosens. Bioelectron.*, 1992, **7**, 411–419.
- 12 E. Zacco, R. Galve, M. P. Marco, S. Alegret and M. I. Pividori, Electrochemical biosensing of pesticide residues based on affinity biocomposite platforms, *Biosens. Bioelectron.*, 2007, **22**, 1707–1715.
- 13 M. Salmain, N. Fischer-Durand and C. M. Pradier, Infrared optical immunosensor: Application to the measurement of the herbicide atrazine, *Anal. Biochem.*, 2008, **373**, 61–70.
- 14 S. Hleli, C. Martelet, A. Abdelghani, N. Burais and N. Jaffrezic-Renault, Atrazine analysis using an impedimetric immunosensor based on mixed biotinylated self-assembled monolayer, *Sens. Actuators, B*, 2006, **113**, 711–717.
- 15 A. Raksha, K. K. Mishra and N. Bharadvaja, in *Biogenic Nanomaterials for Environmental Sustainability: Principles, Practices, and Opportunities*, ed. K. L. P. S. Maulin and N. Bharadvaja, Springer International Publishing, Cham, 2024, pp. 1–11.
- 16 E. Valera, J. Ramón-Azcón, Á. Rodríguez, L. M. Castañer, F. J. Sánchez and M. P. Marco, Impedimetric immunosensor for atrazine detection using interdigitated  $\mu$ -electrodes (ID $\mu$ E's), *Sens. Actuators, B*, 2007, **125**, 526–537.
- 17 Á. Rodríguez, E. Valera, J. Ramón-Azcón, F. J. Sanchez, M. P. Marco and L. M. Castañer, Single frequency impedimetric immunosensor for atrazine detection, *Sens. Actuators, B*, 2008, **129**, 921–928.
- 18 J. Ramón-Azcón, E. Valera, Á. Rodríguez, A. Barranco, B. Alfaro, F. Sanchez-Baeza and M. P. Marco, An impedimetric immunosensor based on interdigitated microelectrodes (ID $\mu$ E) for the determination of atrazine residues in food samples, *Biosens. Bioelectron.*, 2008, **23**, 1367–1373.





- 19 R. Zeng, M. Qiu, Q. Wan, Z. Huang, X. Liu, D. Tang and D. Knopp, Smartphone-Based Electrochemical Immunoassay for Point-of-Care Detection of SARS-CoV-2 Nucleocapsid Protein, *Anal. Chem.*, 2022, **94**(43), 15155–15161.
- 20 S. Madhurantakam, J. B. Karnam, V. N. Dhamu and S. Seetaraman, M. A. Gates- Hollingsworth, D. P. AuCoin, D. V. Clark, K. L. Schully, S. Muthukumar and S. Prasad, Electrochemical Immunoassay for Capturing Capsular Polysaccharide of Burkholderia pseudomallei: Early Onsite Detection of Melioidosis, *ACS Infect. Dis.*, 2024, **10**(6), 2118–2126.
- 21 Z. Yu, J. Tang, M. Xu, D. Wu, Y. Gao, Y. Zeng, X. Liu and D. Tang, Multi-Enzyme Cascade Nanoreactors for High-Throughput Immunoassay: Transitioning Concept in Lab to Application in Community, *Anal. Chem.*, 2024, **96**(28), 11463–11471.
- 22 S. Cosnier, *Electroanalysis*, 2005, **17**, 1701–1715.
- 23 N. Haddour, S. Cosnier and C. Gondran, Electrogenation of a poly(pyrrole)-NTA chelator film for a reversible oriented immobilization of histidine-tagged proteins, *J. Am. Chem. Soc.*, 2005, **127**, 5752–5753.
- 24 K. K. Mishra, V. N. Dhamu, D. C. Poudyal, S. Muthukumar and S. Prasad, PathoSense: a rapid electroanalytical device platform for screening Salmonella in water samples, *Microchim. Acta*, 2024, **191**(3), 146.
- 25 B. Jagannath, S. Muthukumar and S. Prasad, Electrical double layer modulation of hybrid room temperature ionic liquid/aqueous buffer interface for enhanced sweat based biosensing, *Anal. Chim. Acta*, 2018, **1016**, 29–39.
- 26 D. C. Poudyal, V. N. Dhamu, M. Samson, S. Malik, C. S. Kadambathil, S. Muthukumar and S. Prasad, How safe is our food we eat? An electrochemical lab-on-kitchen approach towards combinatorial testing for pesticides and GMOs; A case study with edamame, *Ecotoxicol. Environ. Saf.*, 2023, **252**, 114635.
- 27 D. C. Poudyal, V. N. Dhamu, A. Paul, M. Samson, S. Muthukumar and S. Prasad, A novel single step method to rapidly screen for metal contaminants in beverages, a case study with aluminum, *Environ. Technol. Innovation*, 2022, **28**(A1937), 102691.
- 28 A. Wilkowska and M. Biziuk, *Food Chem.*, 2011, **125**, 803–812.
- 29 Z. Qiu, D. Tang, J. Shu, G. Chen and D. Tang, Enzyme-triggered formation of enzyme-tyramine concatamers on nanogold-functionalized dendrimer for impedimetric detection of Hg(II) with sensitivity enhancement, *Biosens. Bioelectron.*, 2015, **75**, 108–115.
- 30 A. S. Tanak, B. Jagannath, Y. Tamrakar, S. Muthukumar and S. Prasad, Non-faradaic electrochemical impedimetric profiling of procalcitonin and C-reactive protein as a dual marker biosensor for early sepsis detection, *Anal. Chim. Acta*, 2019, **3**(3), 100029.
- 31 J. S. Daniels and N. Pourmand, *Electroanalysis*, 2007, **19**, 1239–1257.
- 32 K. K. Mishra, V. N. Dhamu, C. Jophy, S. Muthukumar and S. Prasad, Electroanalytical Platform for Rapid E. coli O157:H7 Detection in Water Samples, *Biosensors*, 2024, **14**, 298.
- 33 D. C. Poudyal, V. N. Dhamu, M. Samson, S. Muthukumar and S. Prasad, Pesticide analytical screening system (PASS): A novel electrochemical system for multiplex screening of glyphosate and chlorpyrifos in high-fat and low-fat food matrices, *Food Chem.*, 2023, **400**, 134075.
- 34 S. Madhurantakam, J. B. Karnam, S. Muthukumar and S. Prasad, COVID severity test (CoST sensor)—An electrochemical immunosensing approach to stratify disease severity, *Bioeng. Transl. Med.*, 2023, **8**(5), e10566.

